

Manipulative resonant nonlinear optics: nonlinear interference effects and quantum control of nonlinearity, dispersion, transparency and inversionless amplification in an extended strongly-absorbing inhomogeneously-broadened medium

A. K. Popov,^{1,2,*} S. A. Myslivets,² and Thomas F. George^{3,†}

¹*Department of Physics & Astronomy and Department of Chemistry,
University of Wisconsin-Stevens Point, Stevens Point, WI 54481, USA*

²*Institute of Physics of the Russian Academy of Sciences, 660036 Krasnoyarsk, Russia*

³*Department of Chemistry & Biochemistry and Department of Physics & Astronomy,
University of Missouri-St. Louis, St. Louis, MO 63121, USA*

(Dated: July 29, 2004)

Specific features of nonlinear interference processes at quantum transitions in near- and fully-resonant optically-dense Doppler-broadened medium are studied. The feasibility of overcoming of the fundamental limitation on a velocity-interval of resonantly coupled molecules imposed by the Doppler effect is shown based on quantum coherence. This increases the efficiency of nonlinear-optical processes in atomic and molecular gases that possess the most narrow and strongest resonances. The possibility of all-optical switching of the medium to opaque or, alternatively, to absolutely transparent, or even to strongly-amplifying states is explored, which is controlled by a small variation of two driving radiations. The required intensities of the control fields are shown to be typical for cw lasers. These effects are associated with four-wave mixing accompanied by Stokes gain and by their interference in fully- and near-resonant optically-dense far-from-degenerate double-Lambda medium. Optimum conditions for inversionless amplification of short-wavelength radiation above the oscillation threshold at the expense of the longer-wavelength control fields, as well as for Raman gain of the generated idle infrared radiation, are investigated. The outcomes are illustrated with numerical simulations applied to sodium dimer vapor. Similar schemes can be realized in doped solids and in fiber optics.

PACS numbers: 32.80.Qk, 42.50.Gy, 42.50.Hz, 42.50.Ct, 42.79.Ta

I. INTRODUCTION

In the early stages of the laser era four decades ago, the major problem was extracting coherent optical electromagnetic radiation from incoherently-excited materials. The contemporary trend is the inverse, i.e., control of physical properties of materials by coherence injected with lasers. In such a context, this paper is aimed at studying the opportunities of manipulating optical and nonlinear-optical properties of materials without changing their composition and structure based on quantum coherence and interference. The phenomena of resonance, Doppler shift of a frequency, coherence and interference are fundamental concepts of physics. Resonance enables one to greatly enhance processes related to oscillations. The strongest resonances in optics are attributed to quantum transitions in free atoms and molecules. However, one of the fundamental limitations of optical physics is that only a small fraction of molecules can be resonantly coupled with coherent radiation concurrently in an inhomogeneously-broadened medium. This paper shows that coherent control enables one to remove such

limitations and thus substantially increase the efficiency of the nonlinear optical processes.

Coherence is an important concept in physics. Coherent oscillations may interfere to give rise to counter-intuitive effects. A common example is a standing light wave:

$$\begin{aligned} y(t) &= y_1(t) + y_2(t) = a \sin(\omega t - kz) + a \sin(\omega t + kz) \\ &= 2a \cos(\omega t) \cos(kz). \end{aligned}$$

By overlapping two coherent light fluxes, one can produce completely-dark spots, instead of achieving doubled illumination, or vice versa, one can achieve a twofold increase of the oscillation amplitude, which in turn yields a four-fold increase in the illumination. The concept of interference, which is a measure of coherence, is applied to oscillations of any nature. Similar effects can be anticipated in regard to oscillations of bound intra-atomic and molecular charges. Since induced periodically-accelerated and decelerated motion of the atomic electrons is responsible for optical process, the question is how to manage destructive interference and completely stop induced oscillations of an optical electron even in the presence of a resonant electromagnetic field. This would mean the decoupling of light and resonant media, vanished absorption and dispersion. Then, if destructive interference is turned into constructive, that would provide for strongly-enhanced coupling.

The basic idea behind such opportunities can be presented as follows. The oscillating dipole moment of the

*Electronic address: apopov@uwsp.edu;
URL: <http://www.kirensky.ru/popov>

†Electronic address: tfgeorge@umsl.edu;
URL: <http://www.umsl.edu/chancellor>

unity volume, $P(t)$, is a driving term in Maxwell's electrodynamic equations that determines the optical properties of the materials. It is proportional to the number density of atoms N and to the induced atomic dipole moment $d(t)$. If, besides the probe radiation $E_p(t)$, an auxiliary strong driving field $E_d(t)$ is turned on [$E_{p,d}(t) = E_{p,d} \exp(i\omega_{p,d}t)$], optical electrons become involved in nonlinear oscillations:

$$P(t) = \chi E_p(t) + \chi^{(3)} |E_d(t)|^2 E_p(t). \quad (1)$$

This equation displays the superposition of two components oscillating with the same frequency. In the vicinity of a resonance, the real and imaginary parts of the susceptibilities can be commensurate. Therefore, one can control the amplitudes and relative phase of the interfering oscillations (i.e., constructive and destructive interference) by varying the intensity and detuning from the resonance of the driving field. In quantum terms, this means that the coupling of light and matter and, therefore, optical properties of the materials, can be controlled through judicious manipulation of the interference of one-photon and multiphoton quantum pathways. Consequently, this enables one to selectively deposit energy in certain quantum states or, alternatively, to convert energy incoherently deposited in specific quantum states into coherent light, while decoupling such radiation from the absorbing atoms at resonant lower levels. As such, spectral structures in the transparency and refractive index can be formed and modified with the aid of the auxiliary control resonant or quasi-resonant radiation.

Coherent quantum control of optical processes has proven to be a powerful tool to manipulate refraction, absorption, transparency, gain and conversion of electromagnetic radiation (for a review see, e.g., [1, 2, 3, 4, 5, 6, 7, 8]). Among the recent achievements are the slowing down of the light group speed to a few m/s, highly-efficient frequency up-conversion, squeezed quantum state light sources and optical switches for quantum information processing on this basis [9, 10, 11, 12, 13, 14, 15], and judicious control and feasibilities of near 100% population transfer between the quantum energy levels [16]. Much interest has been shown in the physics and diverse practical schemes of lasing without population inversion (see, e.g., [1, 2, 3, 4, 5, 6, 7, 17]). Large enhancement of fully-resonant four-wave mixing through quantum control via continuum states has been proposed in [18].

The present paper considers optical processes controlled through "injected" quantum coherence, which is followed by destructive and constructive nonlinear interference effects. The near- and fully-resonant far-from-degenerate double-Lambda scheme is investigated, where inhomogeneous broadening of all coupled (including multiphoton) transitions is accounted for. Analytical solutions for density-matrix elements (level populations and coherences) are found that account for various relaxation channels, incoherent excitation of the coupled levels, and Doppler shifts of the resonances. These shifts depend on

the relative direction of propagation of the coupled waves. The solution is convenient for further numerical analysis and experiments. It is shown that inhomogeneous broadening of Raman transitions, which is inherent for far-from-degenerate schemes, creates important features on quantum interference in resonant schemes. The feasibility of overcoming with the aid of the coherence processes of the seemingly fundamental limitation imposed by the Doppler effect on the velocity-interval of the molecules concurrently involved in resonant nonlinear coupling is shown. Thus, a major part of Maxwell's velocity distribution can be involved in the concurrent interaction that dramatically increases the cross-section of nonlinear-optical processes in warm gases. As an application, the conversion of the easily-achievable long-wavelength gain to a higher frequency interval is explored. It is shown that the most favorable are the optically-dense samples, where the inhomogeneity of the field intensities along the medium imposes other important features that must be accounted for as well. The optimum conditions for the realization of such processes are investigated, and the potential of quantum switching, amplification and lasing without population inversion based on coherent coupling at inhomogeneously-broadened transitions in optically-dense spatially inhomogeneous media is demonstrated with the aid of numerical simulations. Another important outcome investigated in this paper is the feasibility of manipulation of the resonant medium, from becoming almost entirely optically opaque to strongly amplifying via a completely transparent state by only a small variation of the intensity or frequency of one of the lower-frequency control fields and of a large gain for an idler infrared radiation. It is shown that the required conditions can be fulfilled, e.g., in the framework of experiments similar to [19] with sodium dimer vapor. The important features of both the signal and idler radiation inherent for such a scheme include entangled states and suppression of quantum noise.

This paper is organized into seven major sections. Section II describes a principal experimental scheme aimed at manipulating optical transparency of initially strongly-absorbing media, and provides a set of equations for coupled electromagnetic waves and their solution for several limiting cases. A corresponding theoretical model and the underlying physics are discussed. Section III gives the density matrix equations. Their solutions related to the problems under consideration are given in Appendix A. The physical principles of manipulating the local absorption (amplification) and refractive indices, as well as the principles of eliminating inhomogeneous broadening of nonlinear resonances, are described in Sec. IV. Results of numerical experiments towards the outlined effects are presented in Sec. V. The emphasis is placed on optical switching and amplification without population inversion in an optically-dense medium assisted by Stokes gain, as well as on the optimal conditions to achieve the effects. Section VI outlines earlier experiments on quantum control based on constructive

and destructive interference and is to show a great variety of applications of similar schemes of quantum control. These include up-conversion of infrared, and generation of short-wavelength VUV radiation, selective detection of relaxation processes and weak electric and magnetic dc fields, as well as selective population of energy levels. Section VII summarizes the main outcomes of the paper.

II. RESONANT FOUR-WAVE MIXING ASSISTED BY STOKES GAIN

Consider a simple experiment designed to explore the manipulation of optical properties through quantum interference based on the experimental setup described in a number of publications on resonant nonlinear optics in sodium vapor (e.g. [19]). Two-atom sodium molecules (dimers), Na_2 , possess an electronic-vibration-rotation spectrum in the near-IR and visible ranges that can be covered with commercial frequency-tunable cw lasers. Figure 1 depicts a relevant partial scheme of energy lev-

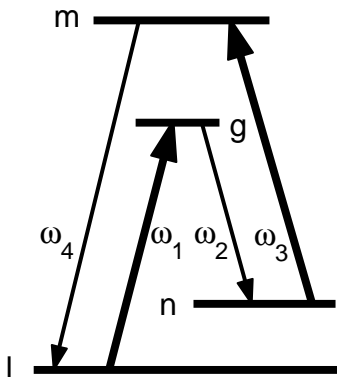


FIG. 1: Optical switching at ω_4 through quantum control by two fields at ω_1 and ω_3 assisted by idler radiation at ω_2 .

els and transitions. Similar schemes are typical for solids doped by rare earths (like Er^{3+} and Pr^{3+}). Assume that the sample is probed with a sufficiently-weak (and thus non-perturbative) optical field in the vicinity of the blue transition ml . Then the refractive and absorption indices in the corresponding frequency interval can be controlled with the driving fields coupled to the lower or upper levels. Resonant driving fields induce back-and-forth transitions with the frequency $G_i = E_i d_{jk} / 2\hbar$ between levels j and k , where G_i (called the Rabi frequency) is the magnitude of the corresponding interaction Hamiltonian scaled to Planck's constant. Modulation of the probability amplitudes leads to a splitting of the resonance at the probe transition and to interference of the one- and two-photon quantum pathways controlled by the driving radiation. This may exhibit itself as odd coherence and interference structures in the absorption and refraction spectra of the probe radiation.

Two independently-varied fields provide for even more

opportunities for manipulating local optical parameters. But three coupled fields, a probe and two driving fields, may generate radiation in the vicinity of the transition gn through four-wave mixing (FWM) processes $\omega_4 + \omega_2 = \omega_1 + \omega_3$. This idler radiation may actually not get depleted but rather substantially enhanced, since the driving field E_1 can easily produce a large Stokes gain. This gain, in turn, can be controlled with the driving field E_3 . These processes dramatically change the propagation properties of the probe field, because three fields, enhanced Stokes radiation and two driving fields at ω_2 , ω_1 and ω_3 , contribute back to the probe field through the FWM process. Thus, doubled FWM assisted by Stokes amplification processes opens extra channels for the transfer of energy from the driving fields to the probe one and, consequently, allows control of the transparency of the medium for the probe radiation. Such a process is usually called optical parametric amplification (OPA). However, as shown below, in resonance, one cannot think about the entire process as a sequence of conventional Raman and FWM processes. This would be misleading in predicting and interpreting the relevant experiments. Indeed, the distinguishing differences in the frequency-correlation properties of single- and multiphoton radiation processes dramatically change in strong resonant fields. This leads to a variety of important effects and applications that are discussed below. Thus, the effect under consideration should be viewed as amplification without inversion (AWI) rather than conventional OPA accompanied by absorption and Stokes gain. *The quantum interference involved in resonant schemes plays such a crucial role that thinking about the conversion process under investigation in terms of the Manley-Rowe photon conservation law would be misleading* [20].

The propagation of four coupled optical waves in a resonant medium is described by the set of coupled equations for the waves $(E_i/2) \exp[i(k_i z - \omega_i t)] + c.c.$ ($i = 1...4$) traveling in an optically-thick medium:

$$dE_{4,2}(z)/dz = i\sigma_{4,2}E_{4,2} + i\tilde{\sigma}_{4,2}E_1E_3E_{2,4}^*, \quad (2)$$

$$dE_{1,3}(z)/dz = i\sigma_{1,3}E_{1,3} + i\tilde{\sigma}_{1,3}E_4E_2E_{3,1}^*. \quad (3)$$

Here, $\omega_4 + \omega_2 = \omega_1 + \omega_3$, k_j are wave numbers in a vacuum, $\sigma_j = -2\pi k_j \chi_j = \delta k_j + i\alpha_j/2$, where α_j and δk_j are the intensity-dependent absorption indices and dispersion parts of the wave numbers, $\tilde{\sigma}_4 = -2\pi k_4 \tilde{\chi}_4$ (etc.) is a FWM cross-coupling parameter, and χ_j and $\tilde{\chi}_j$ are the corresponding nonlinear susceptibilities dressed by the driving fields. Amplification or absorption of any of the coupled radiations influences the propagation features of the others. In the following sections, we will account for possible depletion of the fundamental beams along the medium due to absorption. However, qualitative feature of amplification of the probe beam and generation of the idler radiation are seen within the approximation that a change of the driving radiations $E_{1,3}$ along the medium is neglected. This is possible in some cases, e.g., at the expense of the saturation effects. Then the system (2)-(3) reduces to two coupled standard equations of nonlinear

optics for E_4 and E_2 , whereas the medium parameters

are homogeneous along z . The solution is standard:

$$\begin{aligned} E_2^* &= \exp\left(-\frac{\alpha_2}{2}z - \beta z\right) \left\{ E_{20}^* \left[\cosh(Rz) + \frac{\beta}{R} \sinh(Rz) \right] - i \frac{\gamma_2^*}{R} E_{40} \sinh(Rz) \right\}, \\ E_4 &= \exp\left(-\frac{\alpha_4}{2}z + \beta z\right) \left\{ E_{40} \left[\cosh(Rz) - \frac{\beta}{R} \sinh(Rz) \right] + i \frac{\gamma_4}{R} E_{20}^* \sinh(Rz) \right\}. \end{aligned} \quad (4)$$

Here, $R = \sqrt{\beta^2 + \gamma^2}$, $\beta = [(\alpha_4 - \alpha_2)/2 + i\Delta k]/2$, $\Delta k = \delta k_1 + \delta k_3 - \delta k_2 - \delta k_4$, $\gamma^2 = \gamma_2^* \gamma_4$, $\gamma_{4,2} = \chi_{4,2} E_1 E_3$, and E_{20}^* and E_{40} are input values (at $z = 0$). The first terms in the curved brackets indicate OPA, and the second terms the processes of FWM.

If $\Delta k = \delta k_1 + \delta k_3 - \delta k_2 - \delta k_4 = 0$, the input values $I_{4,2} \equiv |E_{4,2}|^2$ at $z = 0$ are $I_{20} = 0$ and $I_{40} \neq 0$, and the absorption (gain) rate substantially exceeds that of the nonlinear optical conversion obtained at the exit of the medium of length L :

$$\begin{aligned} I_4/I_{40} &= \left| \exp(-\alpha_4 L/2) + (\gamma^2/(2\beta)^2) \right. \\ &\quad \times \left. [\exp(g_2 L/2) - \exp(-\alpha_4 L/2)] \right|^2. \end{aligned} \quad (5)$$

Alternatively, if $I_{40} = 0$, $I_{20} \neq 0$,

$$\begin{aligned} \eta_4 = I_4/I_{20} &= (|\gamma_4|^2/(2\beta)^2) \\ &\quad \times |\exp(g_2 L/2) - \exp(-\alpha_4 L/2)|^2. \end{aligned} \quad (6)$$

Here, $\gamma^2 = \gamma_2^* \gamma_4$, $\gamma_{4,2} = \chi_{4,2} E_1 E_3$, $\beta = (\alpha_4 - \alpha_2)/4$, ($|\gamma^2|/\beta^2 \ll 1$), and $g_2 \equiv -\alpha_2$. From (5) and (6), it follows that at relatively small lengths, the FWM coupling may even increase the depletion rate of the probe radiation, depending on the signs of $\text{Im} \gamma_{4,2}$ and $\text{Re} \gamma_{4,2}$. In order to achieve amplification, large optical lengths L and significant Stokes gain on the transition gn ($\exp(g_2 L/2) \gg |(\beta^2/\gamma^2)|$), as well as effective FWM both at ω_2 and ω_4 , are required. As seen from (4),(5) and (6), the evolution of the coupled fields along the medium strongly depends on whether the Stokes field is injected at the entrance to the medium, and if so, on the value of the ratio of the intensities of the input probe and Stokes fields.

III. DENSITY MATRIX EQUATION AND MACROSCOPIC PARAMETERS OF THE MEDIUM

The macroscopic parameters in Eqs. (4) and (5) are convenient for calculations with the density matrix technique, which allows one to account for various relaxation and incoherent excitation processes. The power-dependent susceptibility χ_4 , responsible for absorption and refraction, can be found as

$$P(\omega_4) = \chi_4 E_4, \quad P(\omega_4) = N \rho_{lm} d_{ml} + c.c., \quad (7)$$

where P is the polarization of the medium oscillating with the frequency ω_4 , N is the number density of molecules, d_{ml} is the electric dipole moment of the transition, and ρ_{lm} is the density matrix element. Other polarizations are determined in the same way. The density matrix equations for a mixture of pure quantum mechanical ensembles in the interaction representation can be written in a general form as

$$\begin{aligned} L_{nn} \rho_{nn} &= q_n - i[V, \rho]_{nn} + \gamma_{mn} \rho_{mm}, \\ L_{lm} \rho_{lm} &= L_4 \rho_4 = -i[V, \rho]_{lm}, \quad L_{ij} = d/dt + \Gamma_{ij}, \quad (8) \\ V_{lm} &= G_{lm} \cdot \exp\{i[\Omega_4 t - kz]\}, \quad G_{lm} = -\mathbf{E}_4 \cdot \mathbf{d}_{lm}/2\hbar, \end{aligned}$$

where $\Omega_4 = \omega_4 - \omega_{ml}$ is the frequency detuning from the corresponding resonance; Γ_{mn} - homogeneous half-widths of the corresponding transition (in the collisionless regime $\Gamma_{mn} = (\Gamma_m + \Gamma_n)/2$); $\Gamma_n = \sum_j \gamma_{nj}$ - inverse lifetimes of levels; γ_{mn} - rate of relaxation from level m to n ; and $q_n = \sum_j w_{nj} r_j$ - rate of incoherent excitation to state n from underlying levels. The equations for the other elements are written in the same way.

It is necessary to distinguish the open and closed energy-level configurations. In the open case (where the lowest level is not the ground state), the rate of incoherent excitation to various levels by an external source essentially does not depend on the rate of induced transitions between the considered levels. In the closed case (where the lowest level is the ground state), the excitation rate to different levels and velocities depends on the value and velocity distribution at other levels, which are dependent on the intensity of the driving fields. For open configurations, q_i are primarily determined by the population of the ground state and do not depend on the driving fields. The Doppler shifts of the resonances $\mathbf{k}_i \mathbf{v}$ can be accounted for in the final formulas by substituting Ω_i for $\Omega'_i = \Omega_i - \mathbf{k}_i \mathbf{v}$ (\mathbf{v} is the atomic velocity).

In a steady-state regime, the solution of a set of density-matrix equations can be cast in the following form:

$$\begin{aligned} \rho_{ii} &= r_i, \quad \rho_{lg} = r_1 \cdot \exp(i\Omega_1 t), \quad \rho_{nm} = r_3 \cdot \exp(i\Omega_3 t), \\ \rho_{ng} &= r_2 \cdot \exp(i\Omega_1 t) + \tilde{r}_2 \cdot \exp[i(\Omega_1 + \Omega_3 - \Omega_4)t], \\ \rho_{lm} &= r_4 \cdot \exp(i\Omega_4 t) + \tilde{r}_4 \cdot \exp[i(\Omega_1 - \Omega_2 + \Omega_3)t], \\ \rho_{ln} &= r_{12} \cdot \exp[i(\Omega_1 - \Omega_2)t] + r_{43} \cdot \exp[i(\Omega_4 - \Omega_3)t]. \end{aligned}$$

The density matrix amplitudes r_i determine the absorption/gain and refraction indexes, and \tilde{r}_i determine the

four-wave mixing driving nonlinear polarizations. Then the problem reduces to the set of algebraic equations

$$\begin{aligned}
P_2 r_2 &= iG_2 \Delta r_2 - iG_3 r_{32}^* + ir_{12}^* G_1, \\
d_2 \tilde{r}_2 &= -iG_3 r_{41}^* + ir_{43}^* G_1, \\
P_4 r_4 &= i[G_4 \Delta r_4 - G_1 r_{41} + r_{43} G_3], \\
d_4 \tilde{r}_4 &= -iG_1 r_{32} + ir_{12} G_3 \\
P_{41} r_{41} &= -iG_1^* r_4 + ir_1^* G_4, \\
P_{43} r_{43} &= -iG_4 r_3^* + ir_4 G_3^*, \\
P_{32} r_{32} &= -iG_2^* r_3 + ir_2^* G_3, \\
P_{12} r_{12} &= -iG_1 r_2^* + ir_1 G_2^*, \\
P_1 r_1 &= iG_1 \Delta r_1, P_3 r_3 = iG_3 \Delta r_3, \tag{9}
\end{aligned}$$

$$\begin{aligned}
\Gamma_m r_m &= -2 \operatorname{Re}\{iG_3^* r_3\} + q_m, \\
\Gamma_n r_n &= -2 \operatorname{Re}\{iG_3^* r_3\} + \gamma_{gn} r_g + \gamma_{mn} r_m + q_n, \\
\Gamma_g r_g &= -2 \operatorname{Re}\{iG_1^* r_1\} + q_g, \\
\Gamma_l r_l &= -2 \operatorname{Re}\{iG_1^* r_1\} + \gamma_{gl} r_g + \gamma_{ml} r_m + q_l, \tag{10}
\end{aligned}$$

where $G_1 = -\mathbf{E}_1 \mathbf{d}_{lg}/2\hbar$, $G_2 = -\mathbf{E}_2 \mathbf{d}_{gn}/2\hbar$, $G_3 = -\mathbf{E}_3 \mathbf{d}_{nm}/2\hbar$, $G_4 = -\mathbf{E}_4 \mathbf{d}_{ml}/2\hbar$, $P_1 = \Gamma_{lg} + i\Omega_1$, $P_2 = \Gamma_{ng} + i\Omega_2$, $P_3 = \Gamma_{nm} + i\Omega_3$, $P_4 = \Gamma_{lm} + i\Omega_4$, $P_{12} = \Gamma_{ln} + i(\Omega_1 - \Omega_2)$, $P_{43} = \Gamma_{ln} + i(\Omega_4 - \Omega_3)$, $P_{32} = \Gamma_{gm} + i(\Omega_3 - \Omega_2)$, $P_{41} = \Gamma_{gm} + i(\Omega_4 - \Omega_1)$, $d_2 = \Gamma_{ng} + i(\Omega_1 + \Omega_3 - \Omega_4)$, $d_4 = \Gamma_{lm} + i(\Omega_1 - \Omega_2 + \Omega_3)$, $\Omega_1 = \omega_1 - \omega_{lg}$, $\Omega_3 = \omega_3 - \omega_{mn}$, $\Omega_2 = \omega_2 - \omega_{gn}$, $\Omega_4 = \omega_4 - \omega_{ml}$, $\Delta r_1 = r_l - r_g$, $\Delta r_2 = r_n - r_g$, $\Delta r_3 = r_n - r_m$, $\Delta r_4 = r_l - r_m$.

For a closed scheme, Eq. (10), r_l must be replaced by

$$r_l = 1 - r_n - r_g - r_m. \tag{11}$$

The solution of these equations as applied to the problem under consideration is given in Appendix A.

IV. NONLINEAR INTERFERENCE EFFECTS IN ABSORPTION AND AMPLIFICATION SPECTRA

A. Nonlinear interference effects in three-level schemes

Consider two simple subcases, $G_3 = 0$ (V -scheme) and $G_1 = 0$ (Λ -scheme). From (9), it follows that

$$\begin{aligned}
P_4 r_4 &= i[G_4 \Delta r_4 - G_1 r_{41}], \\
P_{41} r_{41} &= -i[G_1^* r_4 - r_1^* G_4], \tag{12}
\end{aligned}$$

$$\begin{aligned}
P_2 r_2 &= i[G_2 \Delta r_2 + r_{12}^* G_1], \\
P_{12} r_{12} &= -i[G_1 r_2^* - r_1 G_2^*]. \tag{13}
\end{aligned}$$

The structure of (12) and (13) is the same as that of (1): they present the interference of two oscillations.

At $\Gamma_{gm} \rightarrow \infty$ and $\Gamma_{ln} \rightarrow \infty$, the interference disappears. Consequently, the effect of the driving fields reduces to a change in the level populations (optical pumping). Indeed, the two-photon coherences r_{41} and r_{12} are the source of quantum nonlinear interference effects (NIE), which lead to AWI, Autler-Townes splitting of the resonances and to related effects of electromagnetically-induced transparency, coherent population trapping, and to corresponding changes in the refraction index. From (12) or (A1) at $G_3 = 0$, it follows that

$$\begin{aligned}
\frac{\chi_4}{\chi_4^0} &= \frac{\Gamma_4}{P_4} \cdot \frac{\Delta r_4 - g_1 \Delta r_1}{\Delta n_4 (1 + g_4)} \\
&= \frac{\Gamma_4}{\Delta n_4} \cdot \frac{\Delta r_4 P_{41} - (\Delta r_1 |G_1|^2 / P_1)}{P_{41} P_4 + |G_1|^2}, \tag{14}
\end{aligned}$$

$$\begin{aligned}
\frac{\chi_2}{\chi_2^0} &= \frac{\Gamma_2}{P_2} \cdot \frac{\Delta r_2 - g_3 \Delta r_1}{\Delta n_2 (1 + g_2)} \\
&= \frac{\Gamma_2}{\Delta n_2} \cdot \frac{\Delta r_2 P_{12}^* - (\Delta r_1 |G_1|^2 / P_1^*)}{P_{12}^* P_2 + |G_1|^2}. \tag{15}
\end{aligned}$$

Both equations are of similar structures, and we will briefly review major NIE using the example of Eq. (15). The effects of the driving field G_1 contributing to the change of absorption and refraction indices can be classified as: (i) a change of the populations $\Delta r_4 (|G_1|^2)$, dominant at $\Gamma_{41} \Gamma_{gm} \rightarrow \infty$, and (ii) a splitting of the resonance (see the denominator in (14), dominant at $\Delta r_1 = 0$. With an increase in the detuning Ω_1 , one of the components of Autler-Townes splitting determines the ac-Stark shift of the resonance.

As for any interference, NIE cause only redistribution absorption and amplification over the frequency interval (line shape) but do not change the frequency-integrated absorption (amplification). The latter is determined by the population change only: $\int (\chi_4 / \chi_4^0) d\Omega_4 = \pi \Gamma_4 \Delta r_4 / \Delta n_4$. The term in (14) associated with $r_m = n_m$ describes the line shape (probability) of pure emission, where all the rest (at $r_m = 0$) describe pure absorption. Indeed, as was first emphasized in [21, 23], this difference determines NIE in absorption, emission and amplification spectra which enable the *entire elimination of absorption and appearance of transparency at unequal populations of the levels at the probed transition and to amplification without population inversion in some frequency interval(s) at the expense of enhanced absorption in other intervals*. As seen from (14), at $\Omega_4 = \Omega_1 = 0$, the corresponding requirements to achieve transparency and then amplification without a change of sign of Δr_4 are

$$\Delta r_1 |G_1|^2 / \Gamma_{gm} \Gamma_{lg} \geq \Delta r_4. \tag{16}$$

Therefore, owing to NIE, population inversion between the initial and final bare states is not required in order to achieve AWI in this case. The requirements for transparency at unequal populations of levels at the probed resonant transition and that for amplification without population inversion for Ne transitions was investigated

in [24] (see also [25]) during the course of early studies of NIE with He-Ne lasers. Then lasing without population inversion was experimentally realized in [27] in gas discharge at the transition $2s_2-2p_4$ ($\lambda = 1.15 \mu$) of Ne in the presence of the driving field of another He-Ne laser resonant to the adjacent transition $2s_2-2p_1$ ($\lambda = 1.52 \mu$).

It is misleading to think about resonant processes in Λ and V schemes as conventional Raman processes. The amplification and absorption acquire the features of two-photon processes, while the driving field is detuned from resonance and interference between one- and two-photon pathways vanishes. Indeed, at $|\Omega_1| \approx |\Omega_4| \gg \Gamma_1, \Gamma_4$, $|g_4| \ll 1, |g_1| \ll 1$, $P_4 \approx i\Omega_4, P_1 \approx i\Omega_1 \approx i\Omega_4$, one obtains from (14) the equation for the absorption (amplification) index $\alpha(\Omega_4)$ reduced by its value $\alpha^0(0)$ at resonance at $G_1 = 0$:

$$\begin{aligned} \frac{\alpha(\Omega_4)}{\alpha^0(0)} &\approx \frac{\Gamma_4^2 \Delta r_4}{\Omega_4^2 \Delta n_4} - \text{Re} \left\{ \frac{\Gamma_4 (\Delta r_4 g_4 + \Delta r_1 g_1)}{i\Omega_4 \Delta n_4} \right\} \\ &\approx \frac{\Gamma_4^2 \Delta r_4}{\Omega_4^2 \Delta n_4} - \frac{\Gamma_4 \Gamma_{14}}{\Gamma_{14}^2 + (\Omega_4 - \Omega_1)^2} \cdot \frac{|G_1|^2 (\Delta r_1 - \Delta r_4)}{\Omega_4^2 \Delta n_4} \\ &= \frac{\Gamma_{lm}^2 (r_l - r_m)}{(n_l - n_m) \Omega_4^2} \\ &\quad - \frac{\Gamma_{gm} \Gamma_{lm}}{\Gamma_{gm}^2 + (\Omega_4 - \Omega_1)^2} \cdot \frac{|G_1|^2 (r_m - r_g)}{\Omega_4^2 (n_l - n_m)}. \end{aligned} \quad (17)$$

The last terms in (17) describe Raman-like coupling and originate both from the nominator and denominator in Eq. (14). In this case, population inversion between the initial and final bare states ($r_m = n_m > r_g$) is required for amplification of the probe field.

In more detail, the nature of NIE in the context of interference of quantum pathways and modification of the frequency-correlation properties of multiphoton processes in strong resonant fields was discussed in [25, 28, 29]. Numerical examples of AWI, including effects related to the growth of the amplified field, are given in [30] both for open and closed energy level configurations.

B. Quantum coherence and elimination of inhomogeneous broadening of multiphoton transitions with light shifts

As outlined above, two-photon coherence r_{ln} plays a key role in the processes under investigation. The important feature of the far-from-frequency-degenerate interaction is that the inhomogeneous (in our case, Doppler) broadening of a two-photon transition is much greater than its homogeneous width, $\zeta = \Gamma_{ln}/(\Delta_{lg}^D - \Delta_{ng}^D) \ll 1$, where Δ_{lg}^D and Δ_{ng}^D are the Doppler HWHM of the corresponding transition. Therefore, only a ζ fraction of the molecules are resonantly involved in the process. Correspondingly, the magnitude and sign of the multiphoton resonance detunings and, consequently, of the amplitude and phase of the lower-state coherence ρ_{nl} , differ

for molecules at different velocities due to the Doppler shifts. This is not the case in near-degenerate schemes. The interference of elementary quantum pathways, accounting for Maxwell's velocity distribution and saturation effects, results in a nontrivial dependence of the macroscopic parameters on the intensities of the driving fields and on the frequency detunings from the centers of the inhomogeneously-broadened resonances. However, this limitation that seems fundamental can be overcome by a judicious compensation of Doppler shifts with ac-Stark shifts.

Consider the principles of such compensation for the example of the absorption (gain) index α_2 . In order to account for Doppler effects, we must substitute all Ω_j in the above formulas for $\Omega'_j = \Omega_j - \mathbf{k}_j \mathbf{v}$, where \mathbf{v} is the molecular velocity, and then perform velocity integration over a Maxwell distribution. Corresponding factors P_j must be substituted for velocity-dependent factors $P'_j = P_j(\Omega'_j)$. Let us assume all detunings Ω_j , except $\Omega_1 - \Omega_2$, to be much greater than the corresponding transition Doppler widths. Then all factors P'_j and P'_{ij} , except P'_{12} , become independent of v . According to Eq. (15), the dependence of the denominator on velocity is determined by the factor

$$\begin{aligned} P_{12}^* + |G_1|^2 / P_2' &\approx \Gamma_{ln} - i[\Omega_1 - \Omega_2 - (\mathbf{k}_1 - \mathbf{k}_2) \mathbf{v}] \\ &\quad + [|G_1|^2 / (\Gamma_{lg} + i\Omega_1)] - i(|G_1|/\Omega_1)^2 \mathbf{k}_1 \mathbf{v}. \end{aligned} \quad (18)$$

Equation (18) indicates a velocity-dependent broadening ($\text{Re}\{|G_1|^2/P_2'\}$) and shift ($\text{Im}\{|G_1|^2/P_2'\}$) of the resonance that allows one to compensate for the Doppler effect at $(|G_1|/\Omega_1)^2 \mathbf{k}_1 = \mathbf{k}_1 - \mathbf{k}_2$, and therefore all molecules will be uniformly coupled to the two-photon resonance independent of their velocities. Compensation of the Doppler shifts with light shifts was proposed in [28, 31, 32]. Opportunities for great enhancement of various optical processes with this effect were recently investigated in more detail in [33, 34, 35, 36, 37]. We shall illustrate the above considered effects with numerical simulations applied to the experimental scheme described in Sec. II.

V. NUMERICAL SIMULATIONS

As an example, we shall consider the transitions $l - g - n - m - l$ (Fig. 1) as those of sodium dimers Na_2 : $X'\Sigma_g^+(v'' = 0, J'' = 45) - A'\Sigma_u^+(6, 45)(\lambda_1 = 655 \text{ nm}) - X^1\Sigma_g^+(14, 45)(\lambda_2 = 756 \text{ nm}) - B^1\Pi_u(5, 45)(\lambda_3 = 532 \text{ nm}) - X'\Sigma_g^+(0, 45)(\lambda_4 = 480 \text{ nm})$ from the experiment [19]. We shall use the experimental relaxation data: $\gamma_{gl} = 7$, $\gamma_{gn} = 4$, $\gamma_{mn} = 5$, $\gamma_{ml} = 10$, $\Gamma_l = \Gamma_n = 20$, $\Gamma_g = \Gamma_m = 120$, $\Gamma_{lm} = \Gamma_{nm} = \Gamma_{ng} = \Gamma_{lg} = 70$, $\Gamma_{ln} = 20$, $\Gamma_{gm} = 120$ (all in 10^6 s^{-1}). The Doppler width of the transition (FWHM) at the wavelength $\lambda_4 = 480 \text{ nm}$ at a temperature of 410°C used for modelling is approximately equal to 1.7 GHz. Then the Boltzmann population of level n is 1.4% of that of level l . All of this, as well as the inhomogeneity of the material parameters and phase mismatch

Δk , are accounted for in the numerical simulations described below.

A. Manipulating absorption and amplification indices with coherent elimination of Doppler broadening of multiphoton resonances

Figure 2 depicts absorption (upper plots) and Stokes amplification (lower plots) computed at relatively low intensities of the driving fields that are set to the corresponding resonances. Plot (a) corresponds to the conditions at the entrance to the medium, and (b) to the radiation depleted after propagation through the medium length $Z = \alpha_{40}z = 15$, where the OPA of the probe field reaches its maximum (see Fig. 8). As seen from the plots, the depletion gives rise to a dramatic change in the spectral properties of the absorption index for the probe blue field and of the Stokes amplification index. The line shapes do not resemble those for conventional Raman processes. Despite some power-induced depopulation of the lower level, an increase of α_4 occurs in some frequency interval in the vicinity of the transition resonance center at the expense of its decrease in other frequency intervals. For all the figures here and below, Ω_2 is determined by the equation $\Omega_2 = \Omega_1 + \Omega_3 - \Omega_4$.

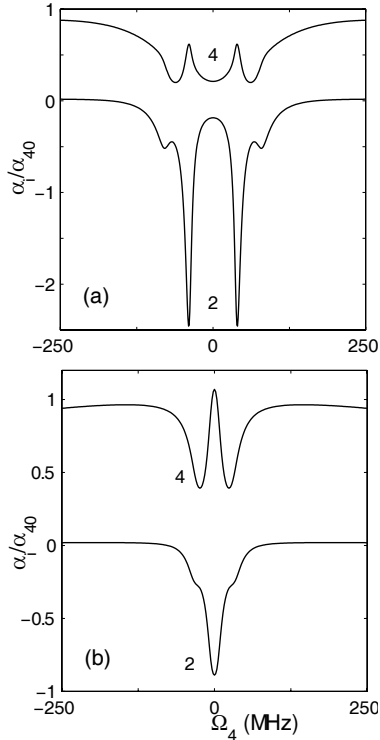


FIG. 2: Spectral structures induced at low intensity of the resonant driving fields. Upper plots - absorption of the probe blue radiation, lower - Stokes gain. $\Omega_1 = \Omega_3 = 0$. (a) $G_1 = 60$ MHz, $G_3 = 20$ MHz; (b) $G_1 = 16$ MHz, $G_3 = 19$ MHz.

Figure 3 displays a substantial inhomogeneity of the

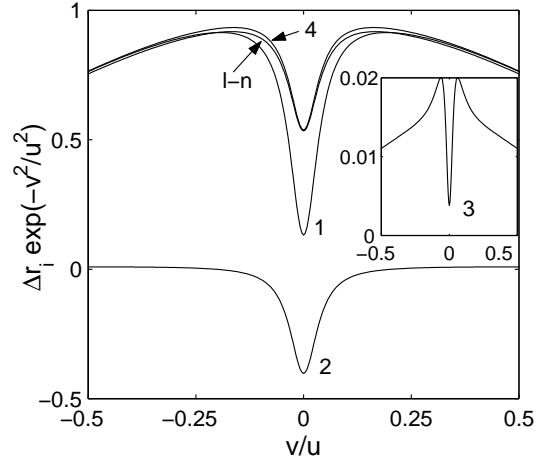


FIG. 3: Differences of level population vs molecule velocity projections v on the wave vectors (u is thermal velocity). $l-n$ corresponds to $r_l - r_n$, and the other plots to the transitions as indicated. All parameters are the same as in Fig. 2(b).

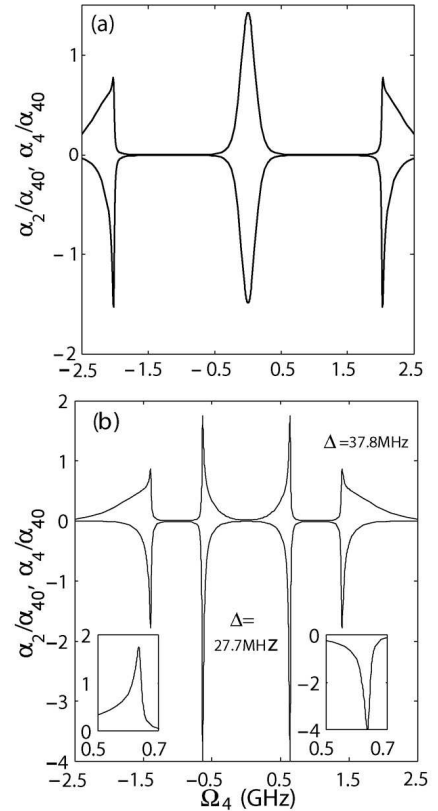


FIG. 4: Resonance laser-induced spectral structures (high intensities of driving fields). Upper plots - absorption of the probe blue radiation, lower - Stokes gain. $G_1 = 1$ GHz, $\Omega_3 = \Omega_1 = 0$. (a) $G_3 = 1070$ MHz, (b) $G_3 = 415$ MHz. Insets - corresponding magnified peaks. Δ - FWHM of the corresponding peaks.

distribution of level populations over the velocities produced by the driving fields. Population inversion appears

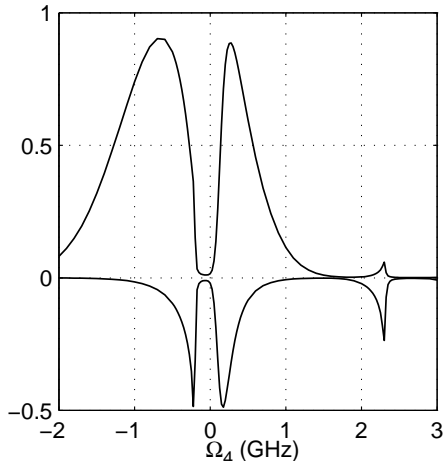


FIG. 5: Laser-induced spectral structures (high intensities of driving fields). Upper plots - absorption of the probe blue radiation, lower - Stokes gain. $G_1 = 1$ GHz, $G_3 = 400$ MHz, $\Omega_1 = 2140$ MHz, $\Omega_3 = 400$ MHz.

at the Stokes transition ng in a narrow velocity interval, while no population inversion is produced at the Raman transition ln . The figure indicates the smallness of the fraction of molecules resonantly coupled to the driving fields. This important fact must be taken into account while considering amplification with and without population inversion [30].

Figure 4(a) shows corresponding line shapes at higher intensities of the driving fields chosen so that the splitting of coupled levels is nearly equal. This determines the coincidence of two out of the four spectral components at the probe and at the Stokes transitions. Plot (b) demonstrates further substantial change of the spectrum by variation of the intensity of one of the fields and appearance of narrow sub-Doppler laser-induced absorption and amplification structures. The position and shape of the structures can be varied within the frequency-interval comparable with the Doppler width.

Figure 5 illustrates the opportunities to form a transparency window in any frequency interval in the vicinity of the probe transition. As follows from Figs. 2, 4 and 5, the maxima and minimum in the Stokes gain, as a rule, correspond to the maxima and the minimum in the absorption index.

Figure 6 demonstrates the feasibilities of compensating for Doppler shifts with ac-Stark shifts and corresponding substantial field-induced narrowing of the induced resonances. The upper plot in 6(a) presents a red-shifted and slightly-decreased Doppler-broadened absorption resonance, and the lower one the feasibility of the formation of a power-induced Doppler-free Stokes resonance. At $G_1^2 \ll \Omega_1^2$, the ac-Stark shift of the Stokes transition is estimated as G^2/Ω_1 , and the dressed two-photon resonance as $\Omega_2 = \Omega_1 + G_1^2/\Omega_1$. This is in a good agreement with the computed plots. The FWHM of the induced resonance is 17 MHz, which is much less than

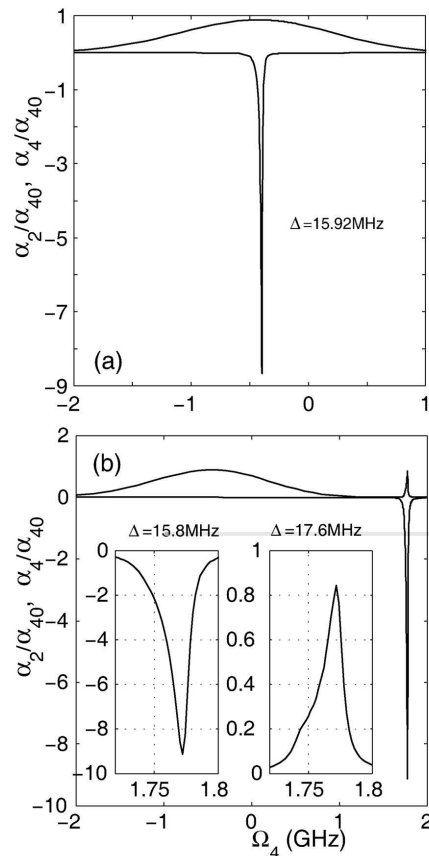


FIG. 6: Compensation of Doppler shifts with light shifts and sub-Doppler resonances. Upper plots - absorption of the probe blue radiation, lower - Stokes gain. $\Omega_1 = 2140$ MHz, $G_1 = 1$ GHz. (a) $G_3 = 0$, ($\Omega_2 = 2140$ MHz - Ω_4); (b) $\Omega_3 = \Omega_1$, $G_3 = 242$ MHz ($\Omega_2 = 4280$ MHz - Ω_4). Δ is FWHM of the corresponding peaks. Insets - magnified corresponding laser-induced structures. The Doppler FWHM of the Raman transition is 170 MHz.

the Doppler FWHM of the Raman transition (170 MHz) and comparable to the homogeneous FWHM of the Raman transition (6.4 MHz). Figure 6(b) shows further feasibilities for producing sub-Doppler structures with two driving fields.

Figure 7 displays the sensitivity of the width of the induced structures on the choice of the parameters of the driving fields. The width of the most narrow resonance (plot 2) is even less than the homogeneous FWHM of the corresponding transitions and commensurate with that of the most narrow resonance in the system (transition ln). Since all nonlinear resonances possess asymmetric and non-Lorentzian shapes, the width of such a resonance has different properties than those attributed to a conventional resonance of a Lorentzian shape. The insets prove that the narrowing is related to judicious compensation of the Doppler shifts by ac-Stark shifts. Plots 2 in the insets indicate that *the central portion of the Maxwell velocity distribution (the majority of atoms)*

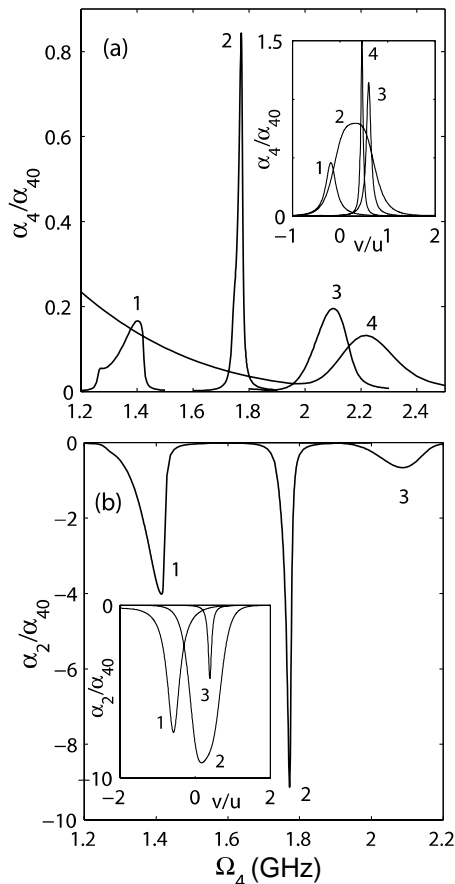


FIG. 7: Power-induced Doppler-free resonances. $\Omega_1 = \Omega_3 = 2140$ MHz, $G_3 = 242$ MHz. (a) - laser-induced structures in absorption index $\alpha_4(\Omega_4)$, inset - velocity distribution $\alpha_4(v/u)$ at Ω_4 set to the center of the corresponding resonance (u is thermal velocity). Maxwell's envelope is removed. Δ - full width at half maximum of the corresponding peaks. (b) - same for Stokes amplification index. (a): 1 — $G_1 = 1500$ MHz ($\Delta = 98$ MHz), 2 — $G_1 = 1000$ MHz ($\Delta = 17.6$ MHz), 3 — $G_1 = 500$ MHz ($\Delta = 133$ MHz), 4 — $G_1 = 0$ ($\Delta = 232$ MHz); (b) - same parameters as in (a), where the FWHM of the structures 1, 2 and 3 are 64, 15.8 and 128 MHz.

becomes involved in the coupling and simultaneously contributes to the absorption maximum of the narrowed resonance (compare with Fig. 3). The other wider resonances remain inhomogeneously broadened.

B. Generation of Stokes radiation, optical switching and inversionless amplification of short-wavelength radiation above the oscillation threshold in resonant optically-dense media

Figure 8 displays the results of numerical simulations of amplification of short-wavelength radiation and of generation of long-wavelength field controlled by quantum interference for the conditions corresponding to Fig. 2. The optimum parameters and output characteristics of

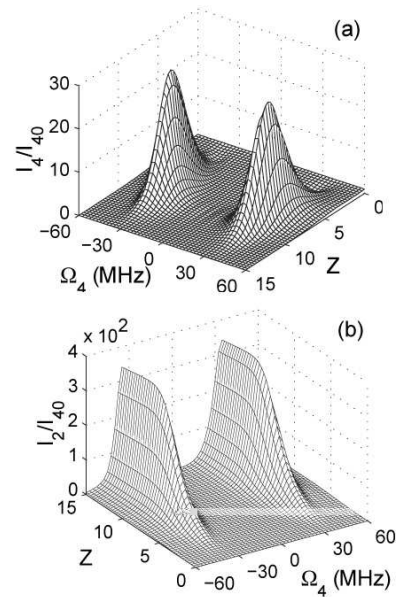


FIG. 8: Laser-induced inversionless amplification, transparency and generated Stokes radiation at low intensities of fundamental beams ($Z = \alpha_{40}z$). $\Omega_1 = \Omega_3 = 0$, $G_{10} = 60$ MHz, $G_{30} = 20$ MHz. (a) probe; (b) generated Stokes idler radiation.

the amplifier are stipulated from the interplay between absorption, amplification of generated idler Stokes radiation [Fig. 8(b)], phase-matching, FWM cross-coupling parameters, and variation of all material parameters along the medium due to saturation effects accounting for the velocity-dependent NIE. It is remarkable that generated idler Stokes radiation may several hundred times exceed the input probe radiation [Fig. 8(b)]. The input Rabi frequencies of the control fields for this graph correspond to the focused cw radiations on the order of several tens of mW, i.e., to about one photon per thousand molecules. The length of the medium is scaled to the absorption length at $\omega_4 = \omega_{ml}$, with all driving fields turned off.

In a good agreement with (5), Fig. 9(a) shows that, first, the probe beam is sharply depleted, and a substantial optical length is required to achieve transparency, and then there is significant inversionless gain (main plot). The complete transparency is achieved at a length of about 4. With the same driving fields but with the probe radiation tuned to the exact resonance (lower right inset), amplification is not achievable. The upper inset shows strong depletion of the driving radiation E_1 along the medium at the chosen intensity and detuning from the resonance. The evolution of the amplitudes of the fields along the medium is determined by the relative phase $\Psi = \phi_4 - \phi_3 + \phi_2 - \phi_1 + (\mathbf{k}_4 - \mathbf{k}_3 + \mathbf{k}_2 - \mathbf{k}_1)_z z = \Theta + \Delta k z$. The lower left inset in Fig. 9(a) shows substantial change of the relative phase Θ along the medium that is determined by the inhomogeneity of the coupled field and, consequently, material parameters. Figure 9(b) presents

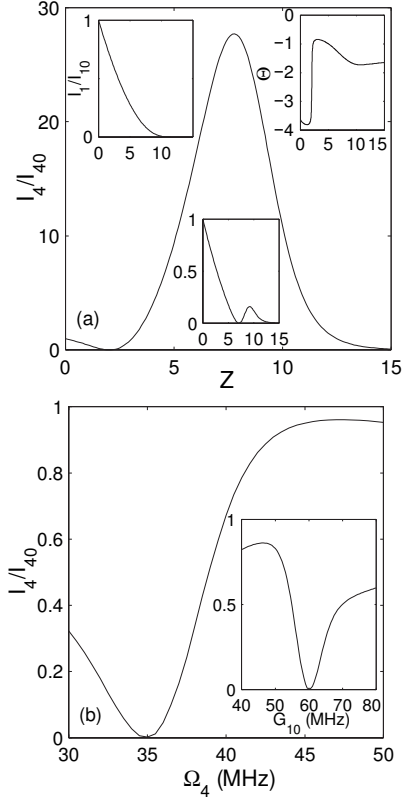


FIG. 9: Propagation of probe radiation (a) and optical switching (b) ($Z = \alpha_{40}z$). $\Omega_1 = \Omega_3 = 0$, $G_{10} = 60$ MHz, $G_{30} = 20$ MHz [(a) and main plot (b)]. (a) $\Omega_4 = 35$ MHz (main plot) and $\Omega_4 = 0$ (lower inset). Upper left inset - depletion of the fundamental radiation at ω_1 , upper right inset - phase for main (a). (b) Main plot and inset - $Z = 2$, inset - $\Omega_4 = 35$ MHz. Minimum transmission is less than 10^{-3} .

feasibilities of all-optical switching, controlled by quantum interference. *Only a small variation of the frequency of the probe field and/or the input intensity of the driving field I_{10} results in a dramatic change of the intensity of the transmitted probe radiation. By this, the sample can be easily driven to the opaque state (less than 10^{-3} of the transparency) or to entire transparency and strong amplification without any change of the level populations.*

Figure 10 displays the change of the number of photons in each beam along the medium scaled to the number of photons in the probe field at the entrance to the medium, assuming $\sigma_i = 0$ in Eqs. (2) and (3). The plots are computed for the same input intensities as Fig. 9(a), but Fig. 10(a) corresponds to the fully-resonant case and Fig. 10 (b) to far-from-resonance coupling. The figure proves that *the interference of quantum pathways plays such an important role in fully-resonant multi-wavelength coupling that the process as a whole can not be viewed as a sequence of independent conventional elementary one-photon/two-photon FWM processes, as they were introduced for off-resonant conditions in the framework of per-*

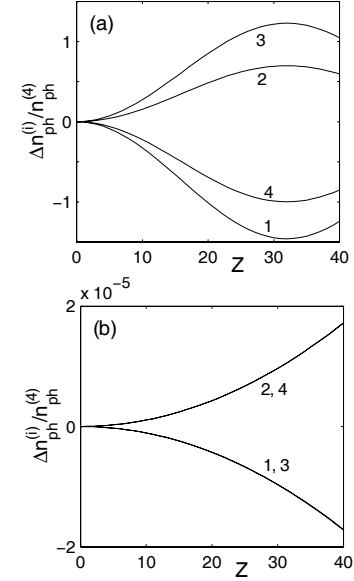


FIG. 10: Relative change of the photon numbers in the coupled fields along the medium at neglected absorption and refraction. $G_{10} = 60$ MHz, $G_{30} = 20$ MHz. (a) $\Omega_1 = \Omega_3 = \Omega_4 = 0$, and (b) $\Omega_1 = 1$ GHz, $\Omega_3 = -1$ GHz, $\Omega_4 = -2.5$ GHz.

turbation theory. Indeed, Fig. 10(a) displays even qualitatively incorrect behavior with respect to the Manley-Rowe relationship (photon conservation law). As detuning from the resonance increases, the disagreement ceases [Figure 10(b)].

Figure 11 shows the feasibility of realizing *strong amplification of the probe short-wavelength radiation at the expense of other longer-wavelength driving radiations, despite the enhanced absorption index.* The importance of optimization of the conversion parameters based on the processes investigated here, on the developed theory and on the numerical simulation is explicitly seen from comparison of the plots (a) and (c). If so, *substantial (several thousand times) amplification of the shortest wavelength radiation becomes feasible.* Amplification slightly exceeding unity ensures generation inside the ring cavity. Hence, Figs. 8, 9 and 11 show feasibilities of *lasing without requirements of population inversion at the resonant transition.*

VI. EARLIER EXPERIMENTS ON RESONANT NONLINEAR-OPTICAL PROCESSES CONTROLLED THROUGH QUANTUM INTERFERENCE

Constructive and destructive nonlinear interference effects, which play a crucial role for quantum switching under consideration in the present paper, are often met and play an important role in nonlinear spectroscopy and in resonant nonlinear optics. Comprehensive experiments on nonlinear interference effects at Doppler-broadened

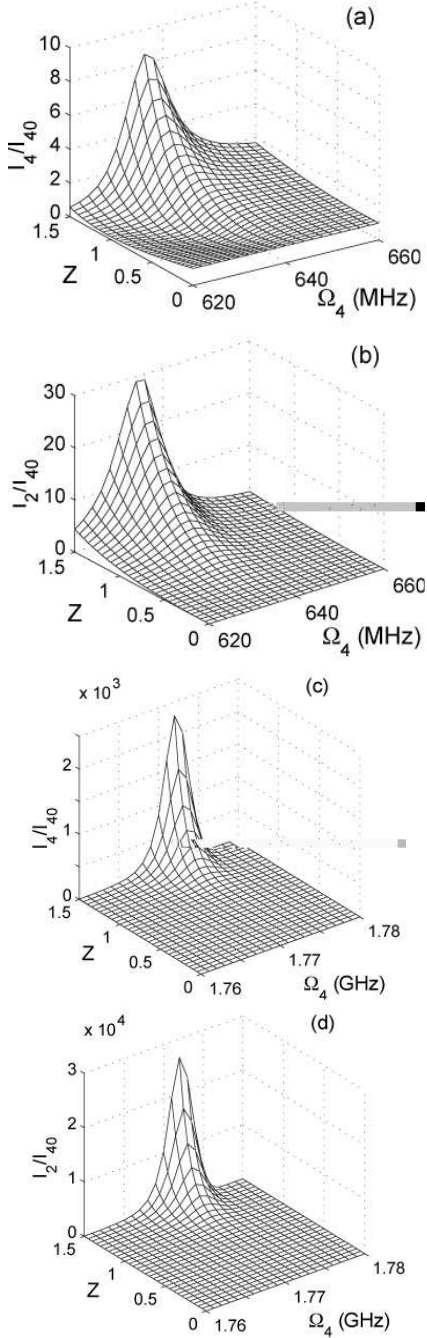


FIG. 11: Laser-induced inversionless amplification, transparency and generated Stokes radiation at higher intensities of fundamental beams. $G_{10} = 1$ GHz. (a) and (b): $\Omega_3 = \Omega_1 = 0$, $G_{30} = 415$ MHz. (c) and (d): $\Omega_3 = \Omega_1 = 2140$, $G_{30} = 242$ MHz.

transitions of Ne in the field of He-Ne lasers had demonstrated feasibilities of producing transparency for cw radiation at the transitions with unequal energy-level populations and lasing without population inversion at the resonant transition [27]. The examples of other early experiments where such interference proved to play a criti-

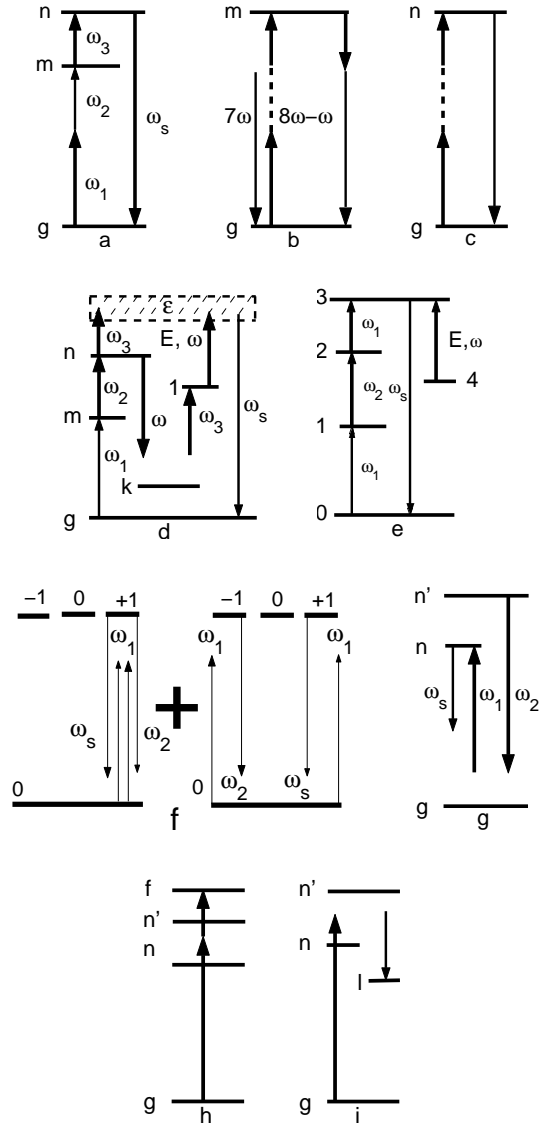


FIG. 12: Interference of quantum pathways and quantum control in resonant nonlinear optics. (a) Up-conversion of infrared radiation ω_2 ; (b) interference of off-resonant 7th-order nonlinear polarization and 9th-order resonant polarization at the generation of the 7th harmonic radiation; (c) interference of resonant one-photon and multiphoton odd-order nonlinear polarization; (d) laser-induced continuum structures (LICS); (e) quantum control of sum-frequency mixing; (f) collision induced four-wave mixing; (g) collision-induced resonance; (h) interference of quantum pathways in two-photon absorption; and (i) interference of quantum pathways in Raman scattering.

cal role are depicted in Fig. 12.

A weak infrared radiation field of arbitrary frequency ω_2 [Fig. 12(a)] can be up-converted by a resonantly-enhanced FWM process in the fields of two frequency-tunable lasers, ω_1 and ω_3 . As confirmed in the experiments on Rb vapors [38], the process that fundamentally limits conversion efficiency is destructive interference of

two components in coherence at transition gm induced by E_1 and E_2 on one hand, and by E_3 and E_s on the other hand.

The interference of two nonlinear-optical processes in Hg vapor [Fig. 12(b)] was employed to prove that direct conversion of intense infrared radiation to VUV by an eight-photon-resonant 9th-order process is more efficient than that with a lower seventh-order but off-resonant process [39]. By a small variation of the eight-photon detuning, destructive interference can be turned to constructive. Thus higher-order resonant polarization component was distinguished and compared with the lower-order off-resonant one.

The interference between linear and nonlinear polarizations [Fig. 12(c)] was shown to limit odd-order resonant harmonic generation and multiphoton resonant ionization (see, e.g. [39] and references therein).

The interference of a one-photon transition to the dissociation or ionization continuum and multiphoton transitions between discrete states through the continuum stipulated by the same probe radiation gives rise to laser-induced continuum structures [40, 41] [Fig. 12(d)]. As was first shown in [42], such laser-induced autoionizing-like structures in the continuum allow one the increase FWM polarization while decrease the absorption of generated short-wavelength radiation. Laser-induced continuum structures enable quantum control of chemical processes related to dissociation and ionization by employing constructive and destructive interference. (For a recent literature survey of the experiments, see [18]). Similar processes can be realized in discrete transitions [Fig. 12(e)].

Figure 12(f) illustrates the FWM process $2\omega_1 = \omega_s + \omega_2$, where E_1 and E_2 are linearly and orthogonal polarized waves with nearly equal frequencies close to the frequency of the transition between non-degenerate level and degenerate level which consist of three Zeeman sub-levels. Linear polarized oscillations can be treated as combinations of two oppositely polarized circular oscillations. Each circularly-polarized component of E_s can be created both due to processes involving photons of the same polarization [left side of Fig. 12(f)] and processes involving photons of opposite circular polarization [right side of Fig. 12(f)]. As was proved in experiments with transitions between excited levels of Ne [43], destructive interference of these two channels eliminate FWM process completely unless specific collisions occur or even very weak magnetic or electric fields are applied. This allows one to selectively detect such collisions among many other relaxation processes as well as to measure the weak fields.

In a similar way, the FWM process presented in Fig. 12(g) does not feel the resonance at $\omega_2 - \omega_1 = \omega_{n'n}$ between excited unpopulated levels unless collisions disbalance the destructive interference in the quantum system [44, 45]. Figures 12(i) and (k) show possible destructive interference of two quantum pathways through intermediate levels n and n' that allows one to control the pro-

cesses of two-photon excitation.

VII. CONCLUSIONS

Specific features of manipulating linear and nonlinear optical properties of resonant materials through constructive and destructive quantum interference in three- and four-level media with *inhomogeneously-broadened multiphoton transitions* are studied. The feasibility of compensating for Doppler-shifts with power-shifts by means of quantum control is shown. This enables the removal of a fundamental limitation on resonant multiphoton coupling with molecules from wide velocity-intervals concurrently independent of Doppler shifts of their resonances and, thus, enables significant increase of the cross-sections of various nonlinear-optical processes in warm gases. Similar effects, with the exclusion of the angular anisotropy of laser-induced nonlinear resonances, are achievable at inhomogeneously-broadened transitions in solids.

The propagation of a probe signal in an extended initially strongly-absorbing resonant sample is investigated, which is controlled by two driving fields through the interference of resonant Raman-type and four-wave mixing processes. *It is shown that under fully- and near-resonant coupling, the interference of quantum pathways usually plays so important a role that the propagation processes as a whole cannot be viewed as a sequence of independent conventional single-photon, multiphoton and FWM processes, as they can be introduced for off-resonant coupling in the framework of perturbation theory.* Substantial differences from the behavior that would be expected based on the concept of linear and nonlinear off-resonance processes is demonstrated through numerical simulations. As regarding the proposed scheme, *it is shown that the entire process cannot be viewed as resonant optical parametric amplification accompanied by Stokes gain and absorption. However, it acquires such features with an increase of resonance detunings.*

Applications to photon switching, frequency-tunable narrow-band filtering, and amplification without population inversion of the probe beam are explored through quantum control by two longer-wavelength fields. Switching to enhanced (practically absolute) opacity or to perfect transparency, or even to amplification without population inversion above the oscillation threshold, is shown to be possible due to quantum interference and to readily-achievable Stokes gain. Such gain appears to be inherent to the far-from-degenerate double-Lambda scheme under consideration. *The feasibilities of manipulating Raman gain for generated idler infrared radiation* are explored too. The outlined processes are associated with the appearance of the complex narrow laser-induced spectral structures in absorption, refraction, Raman, and FWM susceptibilities that vary along the medium. As a rule, a decrease in the absorption index is accompanied by a decrease in local

nonlinear-optical coupling, and vice versa. However, the outlined opportunities of strong amplification becomes possible through the deliberate trade-off optimization.

It is shown that *for fully-resonant fundamental and probe fields, which would correspond to Raman resonance for the generated idler radiation, the probe signal is only depleted.* Because of destructive interference, the rate of depletion may become even higher than that in the absence of the driving fields. On the other hand, *there exist detunings where the initial depletion changes for amplification after propagation through a substantial medium length.* It is shown that one can judiciously select parameters such that the transition from absorption to amplification through complete transparency becomes very sharp. This allows one to vary the transparency of the probe radiation or to switch its transparency between components of wavelength division multiplexing at optical networking by a small variation of intensity and/or detuning of the control fields from resonances. It is shown that *the control can be achieved with the intensities of the driving fields at the level of conventional cw lasers of about one photon per one molecule.* The feasibilities of producing amplification well above the oscillation threshold and of *lasing without population inversion at short-wavelength transitions* at the expense of lower-frequency control fields are demonstrated.

The outcomes are illustrated with numerical experiments. Although the data relevant to most typical and easy-to-realize experiments with sodium molecules have been employed for numerical simulations, similar energy level configurations with inhomogeneously broadened transitions are easily found in rare-earth-doped solids used as Raman amplifiers in optical networking and in quantum nanostructures. Proof-of-principle experiments on fast optical switching based on quantum control and FWM have proven such feasibilities [15]. Since the principles of the proposed switching are based on ground-level coherence, the implementation of spin coherence with the lowest relaxation rate allows one to improve dramatically the performance of such quantum switches.

Acknowledgments

This work was supported in part by DARPA under grant No. MDA 972-03-1-0020. A. K. P. thanks Vladimir

Shalaev for discussions of possible applications of similar schemes of quantum control in nanophotonics.

APPENDIX A: NONLINEAR SUSCEPTIBILITIES AND ENERGY LEVEL POPULATIONS FOR THE CASE WHERE EACH LEVEL IS COUPLED TO ONLY ONE DRIVING FIELD: OPEN AND CLOSED SCHEMES

With the aid of the solution of a set of equations (9) for the off-diagonal elements of the density matrix up to first order in perturbation theory with respect to the weak fields, the equations for the susceptibilities can be presented as [7, 46]

$$\frac{\chi_i}{\chi_i^0} = \frac{\Gamma_i \Delta r_i}{P_i \Delta n_i} (i = 1, 3), \quad \frac{\chi_i}{\chi_i^0} = \frac{\Gamma_i R_i}{P_i \Delta n_i} (i = 2, 4), \quad (\text{A1})$$

$$\tilde{\chi}_2 = -iN \frac{d_{ml} d_{lg} d_{gn} d_{nm} / 8\hbar^3}{d_2 (1 + v_5^* + g_5^*)} \times \left[\left(\frac{\Delta r_1}{P_1 P_{41}^*} + \frac{\Delta r_3}{P_3 P_{43}^*} \right) + \frac{R_4^*}{P_4^*} \left(\frac{1}{P_{41}^*} + \frac{1}{P_{43}^*} \right) \right], \quad (\text{A2})$$

$$\tilde{\chi}_4 = -iN \frac{d_{ml} d_{lg} d_{gn} d_{nm} / 8\hbar^3}{d_4 (1 + v_7^* + g_7^*)} \times \left[\left(\frac{\Delta r_1}{P_1 P_{12}} + \frac{\Delta r_3}{P_3 P_{32}} \right) + \frac{R_2^*}{P_2^*} \left(\frac{1}{P_{12}} + \frac{1}{P_{32}} \right) \right]. \quad (\text{A3})$$

Here $\chi_i^0 = \chi_i(G_i = 0, \Omega_i = 0)$ is a resonance value of the susceptibility for all fields turned off,

$$\begin{aligned} g_1 &= |G_1|^2 / P_{41} P_1^*, g_2 = |G_1|^2 / P_{12}^* P_2, g_3 = |G_1|^2 / P_{12}^* P_1^*, \\ g_4 &= |G_1|^2 / P_{41} P_4, g_5 = |G_1|^2 / P_{43} d_2^*, g_6 = |G_1|^2 P_{41} d_2^*, \\ g_7 &= |G_1|^2 / P_{32}^* d_4^*, g_8 = |G_1|^2 / P_{12}^* d_4^*, v_1 = |G_3|^2 / P_{43} P_3^*, \\ v_2 &= |G_3|^2 / P_{32}^* P_2, v_3 = |G_3|^2 / P_{32}^* P_3^*, v_4 = |G_3|^2 / P_{43} P_4, \\ v_5 &= |G_3|^2 / P_{41} d_2^*, v_6 = |G_3|^2 / P_{43} d_2^*, v_7 = |G_3|^2 / P_{12}^* d_4^*, \\ v_8 &= |G_3|^2 / P_{32}^* d_4^*, \end{aligned}$$

$$R_2 = \frac{\Delta r_2 (1 + g_7 + v_7) - v_3 (1 + v_7 - g_8) \Delta r_3 - g_3 (1 + g_7 - v_8) \Delta r_1}{(1 + g_2 + v_2) + [g_7 + g_2 (g_7 - v_8) + v_7 + v_2 (v_7 - g_8)]}, \quad (\text{A4})$$

$$R_4 = \frac{\Delta r_4 (1 + v_5 + g_5) - g_1 (1 + g_5 - v_6) \Delta r_1 - v_1 (1 + v_5 - g_6) \Delta r_3}{(1 + g_4 + v_4) + [v_5 + v_4 (v_5 - g_6) + g_5 + g_4 (g_5 - v_6)]}. \quad (\text{A5})$$

The populations are described by the formulas below.

OPEN CONFIGURATION:

$$\begin{aligned}\Delta r_1 &= \frac{(1 + \varkappa_3)\Delta n_1 + b_1\varkappa_3\Delta n_3}{(1 + \varkappa_1)(1 + \varkappa_3) - a_1\varkappa_1b_1\varkappa_3}, \\ \Delta r_3 &= \frac{(1 + \varkappa_1)\Delta n_3 + a_1\varkappa_1\Delta n_1}{(1 + \varkappa_1)(1 + \varkappa_3) - a_1\varkappa_1b_1\varkappa_3}, \\ \Delta r_2 &= \Delta n_2 - b_2\varkappa_3\Delta r_3 - a_2\varkappa_1\Delta r_1, \\ \Delta r_4 &= \Delta n_4 - a_3\varkappa_1\Delta r_1 - b_3\varkappa_3\Delta r_3,\end{aligned}\quad (\text{A6})$$

$$\begin{aligned}r_m &= n_m + (1 - b_2)\varkappa_3\Delta r_3, \\ r_g &= n_g + (1 - a_3)\varkappa_1\Delta r_1, \\ r_n &= n_n - b_2\varkappa_3\Delta r_3 + a_1\varkappa_1\Delta r_1, \\ r_l &= n_l - b_1\varkappa_3\Delta r_3 + a_3\varkappa_1\Delta r_1,\end{aligned}\quad (\text{A7})$$

where

$$\begin{aligned}\varkappa_1 &= \varkappa_1^0 \Gamma_{lg}^2 / |P_1|^2, \quad \varkappa_3 = \varkappa_3^0 \Gamma_{mn}^2 / |P_3|^2, \\ \varkappa_1^0 &= 2(\Gamma_l + \Gamma_g - \gamma_{gl})|G_1|^2 / \Gamma_l \Gamma_g \Gamma_{lg}, \\ \varkappa_3^0 &= 2(\Gamma_m + \Gamma_n - \gamma_{mn})|G_3|^2 / \Gamma_m \Gamma_n \Gamma_{mn},\end{aligned}$$

$$\begin{aligned}a_1 &= \frac{\gamma_{gn}a_2}{\Gamma_n - \gamma_{gn}} = \frac{\gamma_{gn}\Gamma_l a_3}{\Gamma_n(\Gamma_g - \gamma_{gl})} = \frac{\gamma_{gn}\Gamma_l}{\Gamma_n(\Gamma_l + \Gamma_g - \gamma_{gl})}, \\ b_1 &= \frac{\gamma_{ml}\Gamma_n b_2}{\Gamma_l(\Gamma_m - \gamma_{mn})} = \frac{\gamma_{ml}b_3}{\Gamma_l(\Gamma_l - \gamma_{ml})} = \frac{\gamma_{ml}\Gamma_n}{\Gamma_l(\Gamma_m + \Gamma_n - \gamma_{mn})}.\end{aligned}$$

CLOSED CONFIGURATION:

In this case, the populations of levels are given by the equations

$$\begin{aligned}\Gamma_m r_m &= w_m r_l - 2 \operatorname{Re} \{iG_3^* r_3\}, \\ \Gamma_g r_g &= w_g r_l - 2 \operatorname{Re} \{iG_1^* r_1\}, \\ \Gamma_n r_n &= w_n r_l + 2 \operatorname{Re} \{iG_3^* r_3\} \\ &\quad + \gamma_{gn} r_g + \gamma_{mn} r_m, \\ r_l &= 1 - r_m - r_g - r_n,\end{aligned}\quad (\text{A8})$$

whose solution is

$$\begin{aligned}r_l &= n_l(1 + \varkappa_3)(1 + \varkappa_1)/\beta, \\ r_g &= (1 + \varkappa_3)[n_l(1 + \varkappa_1) - \Delta n_1]/\beta, \\ r_n &= \{n_m(1 + \varkappa_3)(1 + \varkappa_1) \\ &\quad + [\Delta n_3(1 + \varkappa_1) + \Delta n_1 \gamma_2 \varkappa_1 / \Gamma_n](1 + b\varkappa_3)\} / \beta, \\ r_m &= \{n_m(1 + \varkappa_3)(1 + \varkappa_1) \\ &\quad + [\Delta n_3(1 + \varkappa_1) + \Delta n_1 \gamma_2 \varkappa_1 / \Gamma_n]b\varkappa_3\} / \beta,\end{aligned}\quad (\text{A9})$$

$$\begin{aligned}\Delta r_3 &= r_n - r_m = [\Delta n_3(1 + \varkappa_1) + \Delta n_1 \gamma_2 \varkappa_1 / \Gamma_n] / \beta, \\ \Delta r_1 &= r_l - r_g = \Delta n_1(1 + \varkappa_3) / \beta.\end{aligned}\quad (\text{A10})$$

Here,

$$\begin{aligned}\Delta n_1 &= n_l - n_g, \quad \Delta n_3 = n_n - n_m, \\ n_m &= n_l w_m / \Gamma_m, \quad n_g = n_l w_g / \Gamma_g, \quad n_n = n_l w_n' / \Gamma_n, \\ n_l &= (1 + w_m / \Gamma_m + w_g / \Gamma_g + w_n' / \Gamma_n)^{-1}, \\ w_n' &= w_n + w_g \gamma_{gn} / \Gamma_n + w_m \gamma_{mn} / \Gamma_n, \\ b &= \Gamma_n / (\Gamma_m + \Gamma_n - \gamma_3).\end{aligned}$$

$$\begin{aligned}\varkappa_1 &= \frac{2|G_1|^2}{\Gamma_1 \Gamma_g (\Gamma_1^2 / |P_1|^2)}, \quad \varkappa_3 = \frac{2|G_3|^2 (\Gamma_m + \Gamma_n - \gamma_3)}{\Gamma_m \Gamma_n \Gamma_3 (\Gamma_3^2 / |P_3|^2)}, \\ \beta &= (1 + \varkappa_3)[1 - \Delta n_3 + 2(n_l + n_m)\varkappa_1] \\ &\quad + (1 + 2b\varkappa_3)[\Delta n_3(1 + \varkappa_1) + \Delta n_1 \gamma_2 \varkappa_1 / \Gamma_n].\end{aligned}$$

The remaining notations are as before.

-
- [1] M. O. Scully, Phys. Rep. **219**, 191 (1992).
[2] O. Kocharovskaya, Phys. Rep. **219**, 175 (1992).
[3] P. Mandel, Contemporary Physics **34**, 235 (1993).
[4] M. O. Scully and M. Fleischhauer, Science **63**, 337 (1994).
[5] A. K. Popov and S. G. Rautian, in *ICONO'95: Coherent Phenomena and Amplification without Inversion*, ed. by A. V. Andreev, O. Kocharovskaya, and P. Mandel, SPIE Proc. **2798**, 49 (1996), <http://xxx.lanl.gov/abs/quant-ph/0005114>.
[6] A. K. Popov, Bull. Russian Academy Sci., Physics **60**, 927, 1996 (Allerton Press, New York) [translation from: Izvestiya RAN, ser. Fiz. **60**, 92 (1996)], <http://xxx.lanl.gov/abs/quant-ph/0005108>.
[7] A. K. Popov, in *11th International Vavilov Conference on Nonlinear Optics*, ed. by S. G. Rautian, SPIE Proc. **3485**, 252 (1998), <http://xxx.lanl.gov/abs/quant-ph/0005118>.
[8] S. E. Harris, Physics Today **50** (7), 36 (1997).
[9] A. J. Merriam, S. J. Sharpe, H. Xia, D. Manuszak, G. Y. Yin and S. E. Harris, Opt. Lett. **24**, 625 (1999).
[10] S. E. Harris and L. V. Hau, Phys. Rev. Lett. **82**, 4611 (1999).
[11] S. E. Harris and Y. Yamamoto, Phys. Rev. Lett. **81**, 3611 (1998).
[12] M. M. Kash, V. A. Sautenkov, A. S. Zibrov, L. Hollberg, G. R. Welch, M. D. Lukin, Y. Rostovtsev, E. S. Fry and M. O. Scully, Phys. Rev. Lett. **82**, 5229 (1999).
[13] M. D. Lukin, A. B. Matsko, M. Fleischhauer and M. O. Scully, Phys. Rev. Lett. **82**, 1847 (1999).
[14] A. K. Popov, S. A. Myslivets and T. F. George, Optics Express **7**, 148 (2000); T. F. George and A. K. Popov,

- Optics Letters **25**, 1364, (2000).
- [15] B. S. Ham and P. R. Hemmer, Phys. Rev. Lett. **84**, 4080 (2000).
- [16] T. Rickes, L. P. Yatsenko, S. Steuerwald, T. Halfmann, B. W. Shore, N. V. Vitanov, and K. Bergmann, J. Chem. Phys. **113**, 534 (2000).
- [17] V. Ahufinger, J. Mompert, and R. Corbalan, Phys. Rev. A **61**, 053814 (2000).
- [18] A. K. Popov, V. V. Kimberg, and Thomas F. George, Phys. Rev. A **69**, 043816 (2004).
- [19] U. Hinze, B. N. Chichkov, E. Tiemann and B. Wellegehausen, Opt. Commun. **166**, 127 (1999).
- [20] A. K. Popov, S. A. Myslivets, E. Tiemann, B. Wellegehausen and G. Tartakovskiy, JETP Letters **69**, 912 (1999).
- [21] G. E. Notkin, S. G. Rautian, and A. A. Feoktistov, Sov. Phys. JETP **25**, 1112 (1967).
- [22] T. Ya. Popova and A. K. Popov, Sov. Phys. JETP **25**, 1007 (1967)
- [23] T. Ya. Popova, A. K. Popov, S. G. Rautian and R. I. Sokolovskii, Zh. Eksp. Teor. Fiz. **57**, 850 (1969) [Sov. Phys. JETP **30**, 466 (1970)], <http://xxx.lanl.gov/abs/quant-ph/0005094> .
- [24] T. Ya. Popova and A. K. Popov, Zh. Prikl. Spektrosk. **12**, 989 (1970) [translated into English: Appl. Spectrosc. **12**, 734, (1970)], <http://xxx.lanl.gov/abs/quant-ph/0005047> ; T. Ya. Popova and A. K. Popov, Izv.Vysh. Uchebn. Zaved., Fizika **No. 11**, 38 (1970) [translated into English: Soviet Phys. J. **13**, 1435, (1970)], <http://xxx.lanl.gov/abs/quant-ph/0005049> .
- [25] A. K. Popov, *Introduction to Nonlinear Spectroscopy* (Siberian Branch of Nauka Press, Novosibirsk, 1983), 274 pages (in Russian).
- [26] O. Kocharovskaya and Ya. I. Khanin, Pis'ma v Zh. Eksp. Teor. Fiz. **48**, 581 (1988) [Sov. Phys. JETP Lett. **48**, 630 (1988)].
- [27] I. M. Beterov, *Investigation of Nonlinear Resonant Interaction of Optical Fields in a Three-Level Gas Laser*, Candidate Science Dissertation (Institute of Semiconductor Physics, Siberian Division of the USSR Academy of Sciences, Novosibirsk, 1970).
- [28] T. Ya. Popova, A. K. Popov, S. G. Rautian and A. A. Feoktistov, Zh. Eksp. Teor. Fiz. **57**, 444 (1969) [Sov. Phys. JETP **30**, 243 (1970)], <http://xxx.lanl.gov/abs/quant-ph/0005081> .
- [29] S. G. Rautian and A. M. Shalagin, *Kinetic Problems of Nonlinear Spectroscopy* (Elsevier, Amsterdam, 1991).
- [30] A. K. Popov, V. M. Kuchin and S. A. Myslivets, Zh. Eksp. Teor. Fiz. **113**, 445 (1998) [JETP **86**, 244 (1998)].
- [31] C. Cohen-Tannoudji, Metrologia **13**, 161 (1997).
- [32] C. Cohen-Tannoudji, F. Hoffbeck and S. Reynaud, Opt. Commun. **27**, 71 (1978).
- [33] G. Vemuri, G. S. Agarwal and B. D. Nageswara Rao, Phys. Rev. A **53**, 2842 (1996); **54**, 3695 (1996).
- [34] A. K. Popov and V. M. Shalaev, Phys. Rev. A **59**, R946 (1999).
- [35] A. K. Popov and A. S. Bayev, Phys. Rev. A **62**, 025801, 069901 (2000).
- [36] A. K. Popov, A. S. Bayev, T. F. George and V. M. Shalaev, Europ. Phys. J. – EPJdirect **D 1**, 1 (2000), <http://link.springer.de/link/service/journals/10105/tocs/t0002d.htm> .
- [37] Po Dong, A. K. Popov, S. H. Tang and J. Y. Gao, Opt. Commun. **188**, 99 (2001).
- [38] A. K. Popov, Infrared Physics **25**, 21, (1985).
- [39] V. G. Arkhipkin, and A. K. Popov, Sov. Phys. Usp. **30**, 952 (1987) [translated from Usp. Fiz. Nauk **153**, 423 (1987)].
- [40] Yu. I. Heller and A. K. Popov, *Laser-Induction of Nonlinear Resonances in Continuous Spectra* (Siberian Branch of Nauka Press, Novosibirsk, 1981) 160 pages (in Russian) [translated into English: J. Soviet Laser Res. **6**, N1, 3-84 (1985)].
- [41] P. L. Knight, M. A. Lander, and B. J. Dalton, Phys. Rep. **190**, 1 (1990).
- [42] Yu. I. Heller and A. K. Popov, Opt. Commun. **18**, 449 (1976).
- [43] A. K. Popov and G. Kh. Tartakovskiy, Opt. Commun. **18**, 499 (1976); Im Thek-de, O. P. Podavalova, A. K. Popov, and V. P. Ran'shikov, *ibid* **30**, 196 (1979).
- [44] Y. H. Zou and N. Bloembergen, Phys. Rev. A **34**, 2968 (1986).
- [45] L. Rothberg, in *Progress in Optics*, **24**, 24 (1987), ed. by E. Wolf (North Holland, Amsterdam).
- [46] A. K. Popov and S. A. Myslivets, Kvant. Elektr. **24**(11), 1033 (1997) **25**(2), 192 (1998) [Quantum Electron. **27**(11), 1004 (1997); **28**(2), 185 (1998)].